Appl. Phys. A 36, 1–13 (1985)

Applied Physics A Solids and Surfaces

Dislocation-Related Photoluminescence in Silicon

R. Sauer, J. Weber, and J. Stolz

Physikalisches Institut (Teil 4), Universität Stuttgart, Pfaffenwaldring 57, D-7000 Stuttgart 80, Fed. Rep. Germany

E. R. Weber, K.-H. Küsters, and H. Alexander

Abteilung für Metallphysik im II. Physikalischen Institut, Universität Köln, Zülpicher Strasse 77, D-5000 Köln 41, Fed. Rep. Germany

Received 4 June 1984/Accepted 10 July 1984

Abstract. Photoluminescence is studied in silicon, deformed in a well-defined and reproducible way. Usual deformation conditions (high temperature, low stress) result in sharp spectra of the D1 through D4 lines as recently described in the literature. New lines D5 and D6 emerge for predeformation as above and subsequent low-temperature, high-stress deformation. Another new sharp line, D12, is observed when both the familiar and the novel lines appear simultaneously. Annealing for 1 h at $T_A \gtrsim 300\,^{\circ}\mathrm{C}$ causes all new lines to disappear and the D1–D4 spectra to reappear. Quantitative annealing and TEM micrographs suggest that D5 is related to straight dislocations and D6 to stacking faults, whereas D1–D4 are due to relaxed dislocations. Photoluminescence under uniaxial stress shows that D1/D2 originate in tetragonal defects with random orientation relative to ⟨100⟩ directions, whereas D6 stems from triclinic centers, preferentially oriented – as are the D3/D4 centers. We conclude that the D3/D4 and the D5 and D6 defects are closely related, whereas the independent D1/D2 centers might be deformation-produced point defects in the strain region of dislocations.

PACS: 78.55.–m, 78.55.Ds, 71.55.Fr

Several investigations in the past eight years have documented that dislocations in silicon give rise to characteristic photoluminescence (PL) spectra below the band edge. Drozdov et al. [1] were the first to show in 1976 that four lines are related to dislocations which they labelled D1 (0.812 eV), D2 (0.875 eV), D3 (0.934 eV), and D4 (1.000 eV). Their samples were deformed at 850 °C by bending so that the dislocation density was inhomogeneous along the samples, amounting to about $4 \times 10^7\,\mathrm{cm}^{-2}$ in the central part and being much lower ($\approx 6 \times 10^5\,\mathrm{cm}^{-2}$) at the ends; when the exciting light beam was laterally scanned over the samples they found the intensity of the PL signals to follow the varying dislocation concentration. In a subsequent work [2], the same authors observed that for low dislocation densities ($\lesssim 10^6\,\mathrm{cm}^{-2}$) the D1 and D2 lines became much narrower and exhibited a twofold finestructure. Based on the line shifts under a uniaxial stress, they concluded that D1 and D2 are similar in nature and correspond to bound-to-bound transitions. D3 and D4 which are also similar in their stress response, were concluded to be due to free-to-bound transitions.

The four D lines were not only observed in plastically deformed silicon but were also reported to appear in ion implanted, cw laser annealed silicon by Uebbing et al. [3]. In contrast to the finding of Drozdov et al. that a close interrelation exists between D1 and D2, Uebbing et al. in their spectra found a strong suppression of D_2, and their spectrum was dominated by D1. Gwinner and Labusch [4] investigated silicon plastically twisted at 1000 °C and then annealed at 1150 °C containing a high density of screw dislocations, and reported a broad PL band down to photon

energies of 0.45 eV; in particular, humps were seen on the band at or close to the positions of D1, D2, and D3, D4. They proposed that the absence of strong D1 and D2 luminescence could be due to the bulk excitation of the Nd–YAG laser used, and that the underlying D1 and D2 defects could be associated with dislocations near the surface.

Comparatively extended work has been performed on the characteristic radiative recombination in plastically deformed silicon by Suezava and coworkers [5–8]. They studied the influence of impurities, of annealing, of the deformation temperature and of the dislocation "morphology" on the D1 through D4 lines. Comprehending their results they arrived at the conclusions that 1) impurities and point defect do not play a vital role in the recombination processes under discussion, 2) dislocations themselves are the active recombination centers but dangling bonds are not involved, and 3) D1 and D2 are probably related to geometrical kinks on the dislocations. These authors also concluded from the temperature dependence of the signals that all lines D1 through D4 can be attributed to transitions between shallow levels ($E_i = 4$–7 meV) and deep levels ($E_g - E_i - h\nu$) in the forbidden gap. The influence of oxygen and hydrogen was studied in further works with different or even controversal results. As for oxygen, Drozdov et al. [9] observed an essential broadening of D1 and D2 after 750 °C heat treatment (30 min) of Czochralski-grown ($[O] = 5 \times 10^{17}$ cm^{-3}) silicon deformed at around 700 °C which differed largely in size, however, between D1 and D2; Suezawa et al. [7] reported that D1 does not essentially vary between float-zone and pulled ($[O] = 8 \times 10^{17}$ cm^{-3}) silicon heated at 900 °C, except for a 50% PL intensity reduction for the CZ material at invariant halfwidth. In sharp contrast, Osip'yan et al. [10] found a considerable increase of D1 upon annealing CZ silicon ($[O] > 10^{17}$ cm^{-3}) at ≈ 700 °C which was deformed at 620 °C.

Finally, it was reported by Osip'yan et al. that saturation of compressed crystals with hydrogen entirely extincts the D1 and D2 luminescence lines whereas Gwinner and Kveder [11] observed an enhancement of D1, D2, and D3 after hydrogenation of compressed silicon. A similar result was obtained by Gwinner [12] in twisted silicon, where the D1 line remained unchanged in intensity and the D2 line alone was enhanced by the incorporation of hydrogen into the deformed crystals.

The present work is a study of dislocation-related photoluminescence. Experimental details are given in Sect. 1. In Sect. 2, we describe the basic D1–D4 spectra and the conditions necessary to produce them. Similarly, Sect. 3 is concerned with the novel lines D5, D6, and D12. Temperature controlled PL is reported and discussed in Sect. 4, and Sect. 5 is devoted to uniaxial stress measurements. Section 6 summarizes our essential results and conclusions.

Almost all of our results have been presented at various conferences (without proceedings) and were privatly communicated since 1981; part of the work was briefly published elsewhere [13–15].

1. Experimental

The starting material was floating-zone silicon (etch pit density $\approx 2 \times 10^{14}$ cm^{-2}) which was "undoped" (some 10^{12} cm^{-3} residual boron concentration) or doped with boron or phosphorus up to 10^{16} cm^{-3}. The crystals were deformed in compression along [213], which favors single slip. The overwhelming majority of the dislocations belongs to the primary slip system (burgers vector $\mathbf{b} = 1/2$ [011], glide plane $(1\bar{1}1)$. The deformation geometry is equivalent to the one used by Suezawa et al. [5, 8]. Standard deformations were performed at 650 °C and at variable stress to produce dislocation densities up to some 10^9 cm^{-2}. This procedure results in "relaxed" dislocations as monitored by transmission electron microscopy (TEM) (Fig. 1a). In a second procedure, samples were predeformed at high temperatures (700–850 °C) under low resolved shear stress to produce a certain dislocation concentration. A subsequent low temperature-high stress (LT–HS) deformation changes the dislocation morphology drastically [16] (Fig. 1b): The dislocations are straight and parallel to the ⟨110⟩ directions in the glide plane; smooth curvatures are replaced by sharp bends, thereby decreasing the number of dislocation kinks. The fraction of dislocations with screw character is of the order of 40% instead of 5% in standard deformed crystals. Irrespective of the deformation mode, the dislocations are always dissociated into two Shockley partial dislocations connected by a stacking fault ribbon. The width of this ribbon may be enlarged by LT–HS deformation [16], as will be discussed below.

For our photoluminescence measurements under uniaxial stress, samples are cut from the deformed crystals in small parallelepipeds having typical sizes of $8 \times 2 \times 2$ mm^3 with the long axis parallel to ⟨100⟩, ⟨111⟩ or ⟨110⟩. The samples are immersed in liquid helium and photo-excited by Kr-ion (647 nm), Ar-ion (415 nm) or Nd–YAG (1.064 μm) laser beams. Temperature-controlled experiments are carried out in an evaporation cryostat with the samples cooled in a He vapor stream allowing for optical excitation powers of up to 50 mW. The luminescence light is dispersed by a 1 m grating monochromator (Spex), detected by a cooled Ge-detector (North Coast) and processed by conventional lock-in technique.

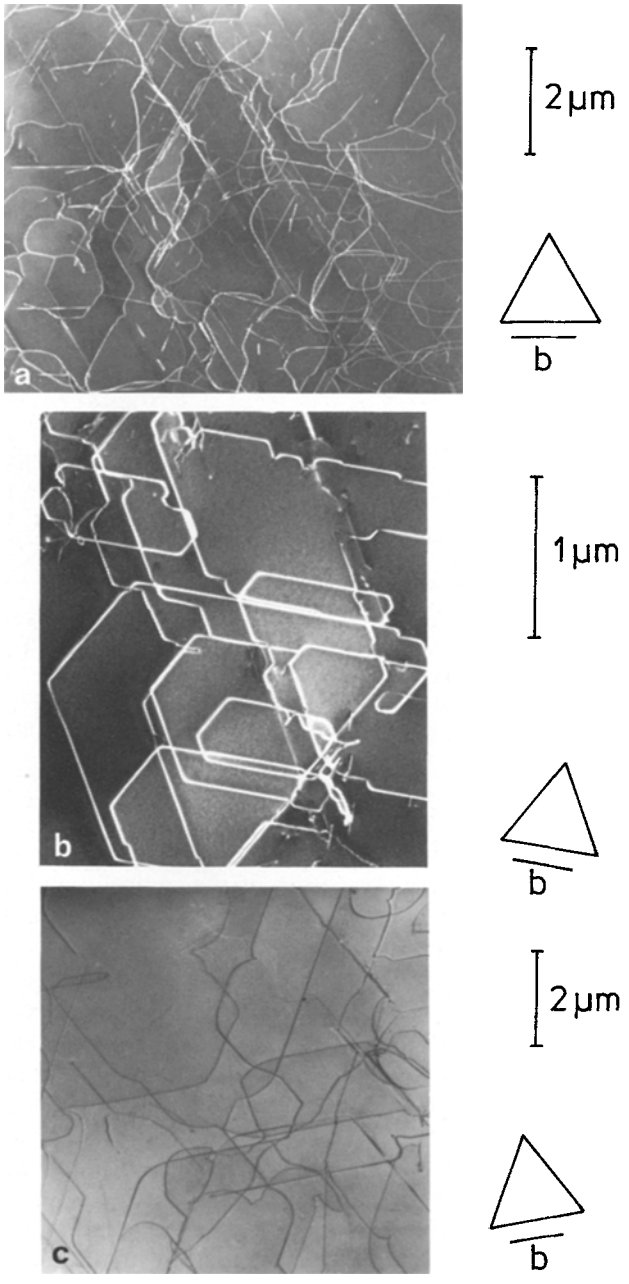

Fig. 1a–c. Transmission electron micrographs of dislocations in silicon crystals deformed by uniaxial compression as specified in Table 1. (a) "Usual" one stage deformation, (b) two stage deformation (LT–HS), (c) two stage deformation (LT–HS) followed by relaxation. The triangles mark the ⟨110⟩ directions in the glide plane, b gives the line of the burgers vector of the primary dislocations. [Micrographs by courtesy of A. Tönnessen (a), E. Heister (b), and F. Sick (c)].

Table 1. Deformation conditions for TEM micrographs in Fig. 1

a) "Usual" deformation: Deformation temperature $T_d = 650\,°C$, resolved shear stress $\tau = 30\,MPa$, deformation time $t_d = 40\,min$, shear strain $\varepsilon = 2.5\%$.

b) Two-stage deformation:
1. Predeformation $T_{d1} = 700\,°C$, $\tau_1 = 19\,MPa$, $\varepsilon_1 = 1.5\%$.
2. LT–HS (low temperature-high stress) deformation $T_{d2} = 420\,°C$, $\tau_2 = 250\,MPa$, $\varepsilon_2 = 0.2\%$, $t_{d2} = 45\,min$.

c) Two-stage deformation followed by relaxation:
1. Predeformation $T_{d1} = 700\,°C$, $\tau_1 = 20\,MPa$, $\varepsilon_1 = 1.7\%$.
2. LT–HS deformation $T_{d2} = 420\,°C$, $\tau_2 = 196\,MPa$, $t_{d2} = 45\,min$.
3. Relaxation by heating without stress up to 330 °C and cooling again without stop.

2. Basic D1 Through D4 Line Spectra

Independent of the method of Drozdov et al. [1] we show that the D1 through D4 lines depend on the existence of dislocations. Whereas these authors measured spatially resolved photoluminescence from heterogeneously dislocated silicon, we record spectra from samples containing homogeneous but different dislocation densities (Fig. 2). The D1 and D2 lines are relatively sharp and exhibit two components split apart by about 5 meV (without external stress) which do not thermalize. The D3 line is much broader showing two unresolved peaks, and the halfwidth of D4 is between those of D1/D2 and D3 (cf. also the spectra shown in Fig. 13). Also visible are phonon-assisted emission lines from free excitons (FE) and electron-hole drops (EHD) [17]. The fine-structure of D1 and D2 has also been reported by Drozdov et al. [2] but was not observed by Suezawa et al. [6]. In our study, the D1 and D2 lines are sometimes split, but often they appear as single lines which in this case are generally broader. We do not find a correlation between the appearance of the fine-structure and the sample doping and preparation. In a similar unexplained manner, the relative intensities of the D lines vary even under nominally identical deformation conditions and seem to be sensitive to details of the preparation procedure. However, the lines D1/D2 and D3/D4 show the same trends whenever spectral changes are observed; they are evidently correlated in pairs in accord with previous observations [2, 8].

When the dislocation density is increased the D line intensities grow clearly supporting the correlation of the lines with the dislocations (Fig. 2). Simultaneously, the near-band gap luminescence (FE, EHD) is effectively quenched. A broad background band develops. We can reach high dislocation densities ($N > 10^9\,cm^{-2}$), where this band dominates the spectrum, lines D1–D4 being only indicated by small humps (Fig. 2). This band is unstable under annealing at 850 °C for about 30 min and is replaced by the D lines (Fig. 3). With respect to the annealing temperature, the band behaves similar to stress-induced paramagnetic pointlike defects observed in EPR [18] and

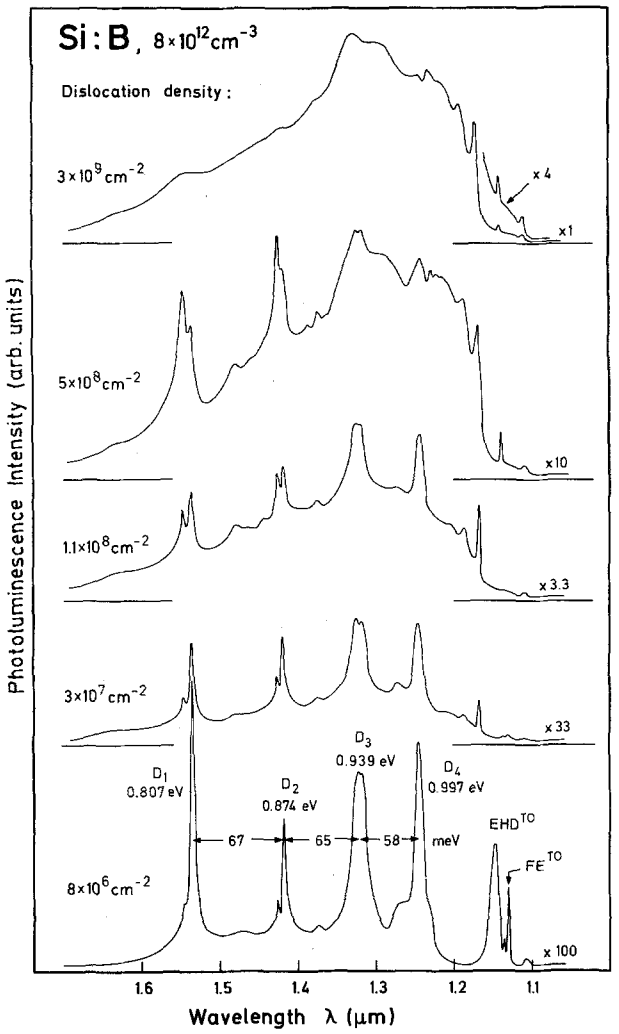

Fig. 2. Photoluminescence spectra from samples deformed at 650 °C along [213] to various dislocation densities as indicated. Bath temperature 4.2 K, resolution $\Delta\lambda = 2$ nm, excitation by 647 nm (≈ 1.92 eV) Kr laser line. Note scale factors for luminescence intensities

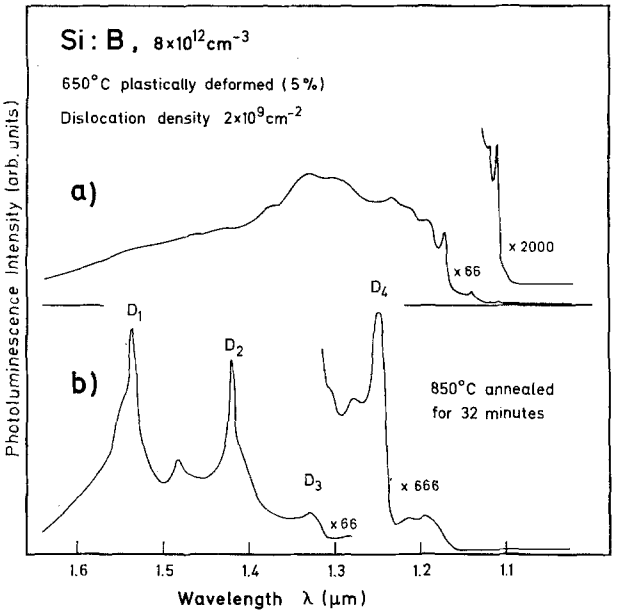

Fig. 3. (a) Broad background spectrum replacing the D lines in highly dislocated silicon (Fig. 2). The sharp high-energy peaks are also typically observed, they are neither familiar extrinsic or intrinsic near band edge features but may be due to point defects introduced along with the dislocations. (b) D line spectrum after 850 °C anneal for about half an hour

may therefore be associated with such EPR centers. The D line spectrum developing after annealing (Fig. 3) exhibits remarkably different intensities of the pairs D1/D2 and D3/D4 in comparison to the spectra of the unannealed samples of low dislocation densities (Fig. 2).

Similar spectra as from samples which are deformed in a well defined way are observed in silicon specimens where dislocations were introduced under various less defined conditions. Some examples are shown in Fig. 4. The main difference is the broader halfwidths of all D lines which is particularly striking for D1/D2, and strongly changing background bands extending from about 1.2 to 1.7 μm. In these examples, D1/D2 clearly dominate over D3/D4. In Fig. 4, the topmost spectrum (a) stems from an initially dislocation-free Tl diffused silicon crystal after Mg diffusion from the gas phase at 1000 °C [19]. The formation of the optically active dislocation states is likely to be due to the diffusion of Mg into the crystals since the primary Tl diffusion alone does not generate this luminescence. (The reason for this observation is not understood.) The intermediate spectrum (b) in Fig. 4 is observed in a float-zone silicon sample after diffusion of oxygen (^{18}O) at 1200 °C to an approximate concentration of 5×10^{17} cm^{-3} [20]. Spectrum (c) in Fig. 4 is measured in some of tiny cylindrical rods of silicon produced by Ar ion laser induced chemical vapor deposition (LCVD) of Si from SiH_4 [21]. Finally, the D line spectrum superimposed on a dominant broad background band is also detected in liquid-phase expitaxial (LPE) silicon layers of 5–10 μm thickness grown from a Bi-rich melt at 950 °C [22]. We further recall as mentioned in the Introduction that the D line spectrum appears in amorphodized and laser-annealed silicon as well as in twisted silicon. Summarizing these observations one concludes: 1) the four D lines are related to the presence of dislocations; 2) their relative intensities can vary to a large extent but D1/D2 and D3/D4 seem to emerge as related pairs; 3) the broad background accompanying the D lines at high dislocation densities has a varying shape depending on the generation procedure of the dislocations, and 4) the four D lines form in the "cleanest" way exhibiting the

smallest halfwidths when the dislocations are introduced by compression along a high-indexed axis (i.e., by single slip).

In the course of the present investigation, we do not find an essential dependence of the D line spectra on doping with donors or acceptors. The D lines are also invariably observed in pulled and float-zoned silicon. This result is consistent with the finding of Suezawa and Sumino [7].

The D line spectrum is sensitive to the penetration depth of the excitation light (Fig. 5). Above-band gap excitation with Ar^+- or Kr^+-ion lasers of slightly phosphorus doped silicon which was deformed at 900 °C to a dislocation density of 3.5×10^7 cm^{-2} yields spectra exhibiting preferentially D1 and D2 at comparable intensities and much weaker the D3 and D4 lines but also comparable in intensity. When the luminescence is excited with a Nd–YAG laser, D3 and D4 remain practically unchanged except that they show weak fluctuations on their shapes; on the other hand, D1 is significantly reduced and D2 is entirely absent from the spectra. Since the exciting photons in the latter case have photon energies $h\nu = 1.165$ eV and E_g (4.2 K) = 1.1695 eV, the excitation is below the band edge E_g, and light absorption is most probably due to a density of states near the band edges induced by the dislocations. The laser penetration depths is of order 1 cm and most of the light is transmitted by the crystal. In the opposite case of Kr laser excitation, the penetration depth is some μm [$\alpha(T < 77\,\text{K}) \approx 10^3$ cm^{-1}].

A possible simple explanation of these data is to assume that D1 and D2 are emitted by dislocation-induced states close to the crystal surface, and D3 and D4 are emitted by dislocation-induced states in the bulk presupposed that the capture efficiency of the photoexcited carriers or the initially formed free excitons is large. In the absence of substantiated values of capture probabilities we may assume efficient trapping of the carriers as the optical centers represent deep electronic states (Sect. 4). Large capture rates may also be concluded from the drastic quenching of the near-band edge luminescence (FE, EHD, and also bound excitons BE) as is obvious from Fig. 2 even at relatively low dislocations densities. The sensitivity of the D1/D2 lines to the excitation wavelength which we find is an accord with the equivalent observation by Suezawa and Sumino [7] when they illuminate their samples with an Ar laser or, alternatively, by 1 μm light from a halogen lamp. These authors, however, excluded the above explanation for several reasons. Either argumentation, however, that of Suezawa et al. as well as our, seems to be not conclusive enough for an unambiguous interpretation of the observed wavelength dependence. Systematic sample thinning with

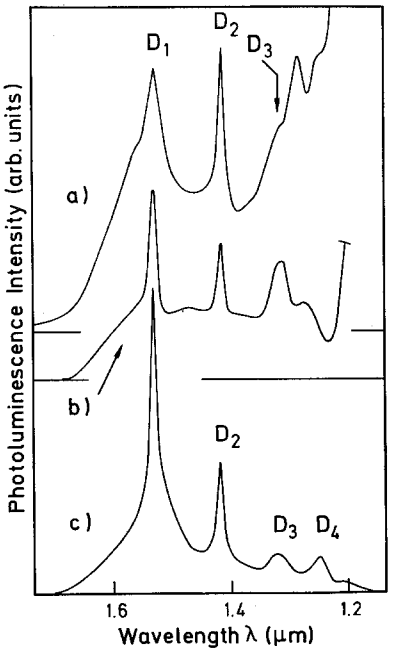

Fig. 4a–c. D line spectra after production of dislocations in different ways: (a) Tl and Mg diffusion into silicon at 1000 °C, (b) oxygen diffusion at 1200 °C for 30 h, (c) growth of silicon rods by LCVD from SiH_4 (see text)

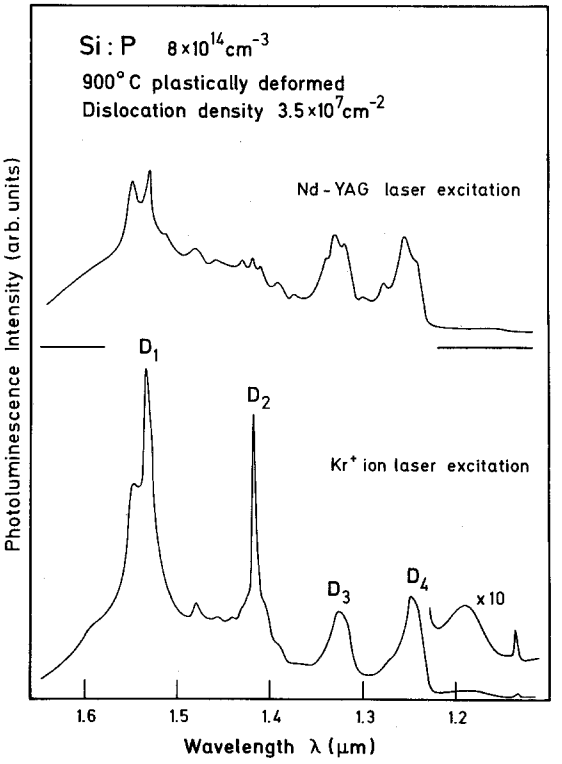

Fig. 5. D line spectra with above – gap excitation ($h\nu = 1.915$ eV, Kr^+ laser) and with below – gap excitation ($h\nu = 1.165$ eV, Nd–YAG laser). Laser power is 400 mW in both cases focused to similar spot sizes on sample (≈2 mm)

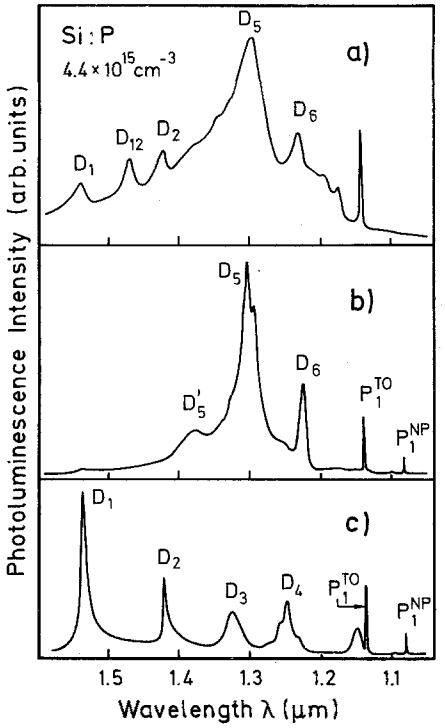

Fig. 6. (a) Spectrum after two-stage deformation. Predeformation: $T_{d1}=650\,°C$, $\tau_1=30$ MPa. LT–HS deformation: $T_{d2}=420\,°C$, $\tau_2=300$ MPa, total $\Delta l/l=0.9\%$; for line D12, see Fig. 8. (b) As (a) but $T_{d1}=850\,°C$, total $\Delta l/l=0.4\%$. The samples contain only straight dislocations, no point-like defects. (c) Same crystal as in (b) after 1 h anneal at 390 °C

large total material removal should be performed as an experimental clue to this open question.

These results may be discussed in conjunction with PL spectra measured for hydrogenated samples. Two specimens from different starting materials exhibited similar spectra after plastic deformation. Both samples were then bombarded by a rf-plasma beam in a quartz tube at constant H_2-gas pressure of 600 Pa containing at least 50% atomic hydrogen. During the total H loading time, the temperature was decreased from 370° to 300 °C in steps of 30 min [23]. After this procedure, the D line spectra showed essentially no alteration except for about 20% changes in the relative intensities. This result is equivalent to the observation of Gwinner [12] that in twisted silicon the same procedure as outlined above leaves the D1 line unchanged in intensity while D2 is enhanced. A third specimen was hydrogen loaded for 7 h with the temperature varied from 400° to 200 °C [24] and led to a marked enhancement of the D1 line in agreement with the very recent finding of Gwinner and Kveder [11]. On the other hand, it has been concluded [11, 25] that the depth of the hydrogenated layer extends to approximately 10–100 μm, and that the hydrogenation passivates electrically active defects associated with dislocations, in particular dangling bond states. Combining the hydrogenation effects and our tentative interpretation of the excitation wavelength effects on the D line spectra we are led to the results that (a) the D1/D2 lines may be due to recombination centers concentrated in a layer some 10 μm beneath the crystal surface and (b) seem to be not related to dangling bonds or other electrically active defects.

3. New Lines D5, D6, and D12

Our standard deformation at low stress and at 650 °C (or at $\geqq 800\,°C$ to avoid the broad background luminescence) gives always rise to the appearance of the lines D1 through D4. Novel luminescence features are obtained when the standard deformation (now to be labeled "predeformation") is followed by a second compression at low temperature (typically 420 °C) and high stress. As mentioned in Sect. 1, the high shear stress enables the dislocations to change their directions rather abruptly by sharp bends. Between these bends the dislocations may follow nearly perfectly the minima of the Peierls potential of the crystal which are parallel to ⟨110⟩ directions [26] (Fig. 1b). Photoluminescence spectra of samples subjected to this treatment are shown in Fig. 6. When the predeformation is performed at 650 °C and the overall deformation is 0.9% we observe a relatively broad new band D5 at about 1.3 μm (≈ 0.953 eV) accompanied by a much narrower line D6 close to 1.224 μm (≈ 1.0126 eV) (Fig. 6a). We observe also an extra very narrow line in Fig. 6a (right hand side). Since it is shifted from P_1^{TO} by ≈ 3 meV to lower energies it is not the transverse optic (TO) replica of the phosphorus bound exciton emission P_1, but is at this high deformation probably due to point defects as are also the remaining relatively sharp features between this line and ≈ 1.2 μm. The novel emission features D5 and D6 can be made even more characteristic by choosing a higher predeformation temperature (850 °C, Fig. 6b) which suppresses the point defect band and related structure. The D5 spectrum is now resolved into two bands, D5 at ≈ 1.3 μm and D5′ at ≈ 1.38 μm (≈ 0.90 eV) which are always simultaneously observed. The D5 line exhibits a fine-structure which is composed of two components in Fig. 6b but is sometimes much more complex (see later). The D6 line now appears on an essentially reduced background, D1 and D2 are absent from the spectra and the appearance of the phosphorus bound exciton lines (P_1^{TO}, P_1^{NP}) indicates a relatively low density of (straight) dislocations. Important is, that the new features D5 and D6 entirely disappear when the samples are annealed for 1 h at a moderate temperature as 390 °C (Fig. 6c). In this case, they are replaced by the familiar lines D1 through D4.

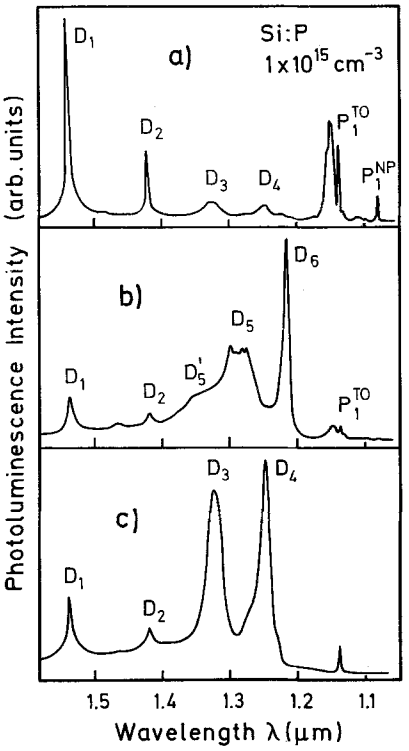

Fig. 7a–c. Spectra of deformed Si:P, 1×10^{15} cm^{-3}. (a) Predeformed crystal: $T_{d1} = 850$ °C, $\tau_1 = 10$ MPa, $\Delta l/l = 0.1\%$, compression axis [213]. (b) Two stage deformation: Predeformation as in (a), LT–Hs deformation: $T_{d2} = 420$ °C, $\tau_2 = 350$ MPa, additional $\Delta l/l = 0.05\%$, compression axis [2, 1, 11], generating high densities of wide stacking faults. (c) Same crystal as in (b) after 1 h anneal at 390 °C

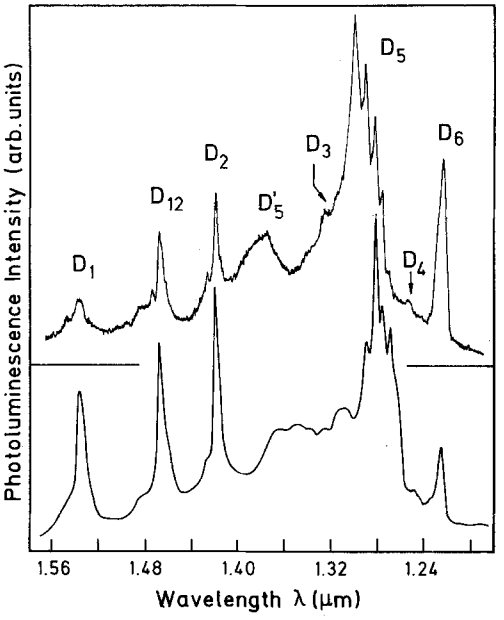

Fig. 8. New line D12 in samples exhibiting D1/D2 *and* D5/D6 simultaneously, and finestructure of D5. *Top spectrum:* Two stage deformation. Predeformation: $T_{d1} = 850$ °C, LT–HS deformation: $T_{d2} = 420$ °C, $\tau_2 = 300$ MPa, $\Delta l/l = 0.4\%$. *Bottom spectrum:* As top spectrum but $T_{d1} = 800$ °C, $\tau_2 = 225$ MPa, $\Delta l/l = 0.45\%$

TEM micrographs of equivalently treated samples show that the straight dislocations have relaxed to curved dislocations. Uniaxial compression along a ⟨213⟩ axis causes the dissociation of most dislocations to become wider which means enlargement of the stacking fault area per unit crystal volume. Therefore we conclude from comparison of PL with TEM that the novel lines D5 and D6 may be related to straight dislocations (preferentially of screw character) and stacking faults.

Based on this still tentative interpretation, one can try to distinguish between effects due to straight dislocations and stacking faults. To this end, we subjected a predeformed sample exhibiting the usual D1–D4 spectrum (Fig. 7a) to a LT–HS deformation along the [2, 1, 11]-direction. This particular treatment results in a high density of straight, *widely* dissociated partial dislocations and therefore, a high density of stacking faults [27]. In the associated spectrum (Fig. 7b), the D6 line has largely increased in comparison to Fig. 6b, and is the dominant feature now. Weaker but still much more intense than the residual D1/D2 emission is the D5 luminescence. This supports our identification of D5 and D6 as being due to straight dislocations. The dominance of D6 over D5 clearly suggests that D6 is related to stacking faults and D5 to straight dislocations. The different nature of the D6 defect states from the D1/D2 states is corroborated by uniaxial stress experiments later in this paper. Again, the novel D5/D6 spectra disappear upon a 390 °C, 1 h anneal of the sample; instead, the D1–D4 spectra emerge with dominating D3/D4 lines. In the TEM micrograph, the straight and widely dissociated dislocations have been replaced by curved dislocations with narrow (≈ 50 Å) stacking faults (Fig. 1c). We summarize our conclusions up to this point: The D1–D4 spectrum is the one which is usually found under "normal" deformation conditions; it is associated with "relaxed", curved dislocations. The D5 and D5′ lines are related to straight dislocations whereas D6 corresponds to stacking faults.

Whenever samples are deformed in a way that the spectra contain both, the D1/D2 and the D5/D6 lines, we observe a further line D12 (Fig. 8) at 1.468 μm (0.8443 eV). This line is not visible (or only extremely weak) when either D1/D2 or D5/D6 are absent from the spectra. Since D5 and D6 are annealed out at 390 °C the samples containing the relaxed dislocations do no longer show D12. Our observations suggest a common parentage of states associated with straight *and* curved dislocations for D12, however, conclusions

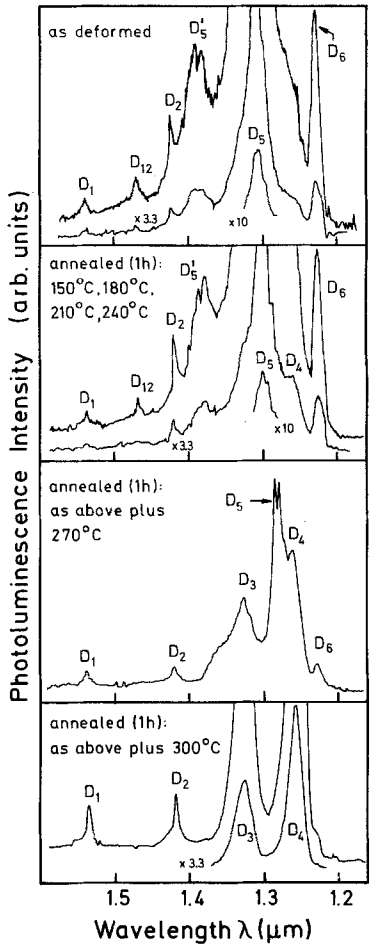

Fig. 9. Dependence of spectra on 1 h isochronal anneal. Two stage deformation. Predeformation: $T_{d1}=850\,°C$, LT–HS deformation: $T_{d2}=420\,°C$, total $\Delta l/l=0.25\%$, compression axis [213] (similar to Fig. 8, top spectrum). The sample was consecutively annealed at the temperatures specified in the diagrams

as to the nature of the D12 defect cannot be drawn at present. Under uniaxial stress (Sect. 5), D12 exhibits shift rates similar to D1 and D2 (although line splittings as for D1 and D2 were not observed) which may indicate a close relation of D12 to the D1 and D2 defects.

Figure 8 reveals also another effect which we observed in many crystals. All samples which have undergone a predeformation at high temperatures show the D5 line split into several components which sometimes can be clearly resolved. The number of components and their relative intensities (which vary to a great extent) depend on the specific preparation conditions in a way which is not yet understood; on the other hand, the positions of the finestructure components are apearently independent of the preparation. From the sample data given in Fig. 8 one may read off the trend that higher total deformation favors the center-of-gravity to shift to higher energies. Although this trend is supported by some more samples and spectra, the effect has no further been investigated in the present work.

The annealing behavior of the novel D5 and D6 lines has been studied in more detail (Fig. 9). Isochronal, 1 h annealing under Ar buffer gas does not affect the lines up to 240 °C. From a temperature of between 240° and 270 °C, D12 disappears and D5 starts to decrease shifting simultaneously to higher energies, and D6 also becomes weaker. At 300 °C, D5 can no longer be detected as it is close to the position of D4 which was greatly enhanced between 270° and 300 °C. A residual weak hump of D6 can be detected after 300 °C annealing. A second sample prepared from different starting material and exhibiting initially the same spectrum as the sample in Fig. 9 was subjected to the same annealing steps; some more steps, however, were inserted between 270° and 300 °C. In this case, even after 290 °C annealing we find weak remainders of D5 and D6. This annealing behavior is similar to that of widely dissociated dislocations as observed by TEM [28] where the relaxation of the straight dislocations takes place between 270° and 350 °C (there within 10 min, Fig. 1c).

The comparison of photoluminescence observations and dislocation morphology as revealed by TEM cannot be pushed to a quantitative level because of the lack of information on radiative quantum efficiencies and carrier capture cross sections of the D1–D4 centers as well as of the D5 or D6 centers. Those parameters being unknown it is impossible to calculate numbers of dislocation states belonging to a certain PL line intensity. Keeping this in mind, we just state that annealing for time intervals of the order of an hour between 270° and 300 °C simultaneously changes dislocation morphology and PL spectra: Transformation of straight dislocations with wide stacking fault ribbons into curved dislocations with narrow stacking faults is accompanied by transformation of the D5/D6 lines into the D1/D2 and D3/D4 lines.

4. Thermal Data on D1–D4

The temperature dependence of the luminescence lines D1 through D4 was measured from 4.2 K up to 200 K (Fig. 10). Two characteristic dependences were observed. D1 and D3 remain virtually constant up to 20 K and are then rapidly deactivated with about 10 meV. D2 and D4 show a gradual decrease even at low temperatures which finally turns into a quenching with about 10 meV deactivation energy. As there are no vibronic sidebands associated with the dislocation luminescence, and as we have not detected excited (electronic) states of the D lines in the temperature-controlled experiments we may assume that the

thermal quenching energy corresponds to dissociation of the upper defect states and is not caused by vibronic coupling. This interpretation places the upper luminescent states as close as some meV to the conduction or valence band. The spectroscopic displacement energies from the band edge E_g which reflect the total binding energy of the luminescing localized electron hole pairs are substantially larger than the corresponding dissociation energies suggesting that *one* particle is weakly bound and thermally released; the remaining particle resides in a deep level in the forbidden gap essentially corresponding to the transition energies, $(E_c - h\nu)$ or $(E_v + h\nu)$. Possibly the shallow states are split from the nearby band by the long-range strain field of the dislocations [29]. Very much differing thermal and spectroscopic binding energies have been reported and discussed in the literature in several other cases of optically active deep centers in silicon [14, 30].

The intensities of D1/D3 and D2/D4 show a parallel development in Fig. 10. To concentrate on D1 and D2, the particular temperature dependence of the D2 line is characteristic of the dissociation of bound electron-hole pairs into a band which is described by an expression

$$I(T)/I(0) = [1 + gT^{3/2} \exp(-E/kT)]^{-1}. \quad (1)$$

Here the continuous density-of-states in the band is accounted for by the term $gT^{3/2}$ which is proportional to the ratio of the degeneracy factor of the bound state and the effective density of states in the band, and E is the dissociation energy. The above expression is a simple generalization [31] of the familiar formula

$$I(T)/I(0) = [1 + g^* \exp(-E/kT)]^{-1}, \quad (2)$$

which describes the thermal partition of localized electron-hole pairs between different bound states of the same center, to bound-to-free thermal activation. The second, basic formula is obtained when under stationary conditions the total generation rate is balanced by the decay rates from the different bound levels. Then g^* incorporates the ratio of the associated degeneracy factors and the inverse ratio of the radiative lifetimes of the involved states. Equation (1) fits the D2 temperature dependence in Fig. 10 with a value of $E = 1$–2 meV, much lower than obtained from simple inspection of the thermal data in Fig. 10. D1 in comparison is better fitted by (2) applying to bound-to-bound thermal activation. However, the data are not sufficiently accurate to exclude a bound-to-free model for D1 with an activation energy close to 10 meV.

We will not lay stress on the quantitative aspects but emphasize that the transition upper states of D1 and D2 are definitely *different*. We combine this statement with other findings. The uniaxial stress results anticipated here from Sect. 5 strongly suggest that D1 and D2 are transitions at the same defect since the lines split or shift identically under stress. However, the different initial states of the D1 and D2 transitions do not thermalize and the lines are observed in very different intensity ratios after various production conditions of the dislocations, as outlined in the Introduction. Possible explanations are that the defect exists in two modifications with minor differences in the elastic properties but distinct differences in the electronic levels, or the upper defect states of D1 and D2 represent different electronic configurations of the same defect interacting via a potential barrier of some meV which prevents (quasi-) thermal equilibrium between the states. The latter model seems to be objectionable as it does not explain the largely varying D1-to-D2 intensity ratios in different crystals. For D3 and D4, comparing the stress data and thermal data, we may correspondingly conclude that also in this case the luminescent defect exists in two modifications with similar energetic positions of their upper states to the D1 and D2 defects. This would be a surprising result in view of the greatly differing properties of the D3 and D4 defects as to symmetry and orientation in the lattice (see below).

We note that similar data to ours were obtained by Suezawa and Sumino [8] for D1 and D2 in heavily dislocated CZ silicon. In their interpretation, they considered one mobile particle bound to a shallow defect state and a second particle (of opposite charge) bound to a deep defect state. Separately formulating occupation numbers for the shallow and deep levels

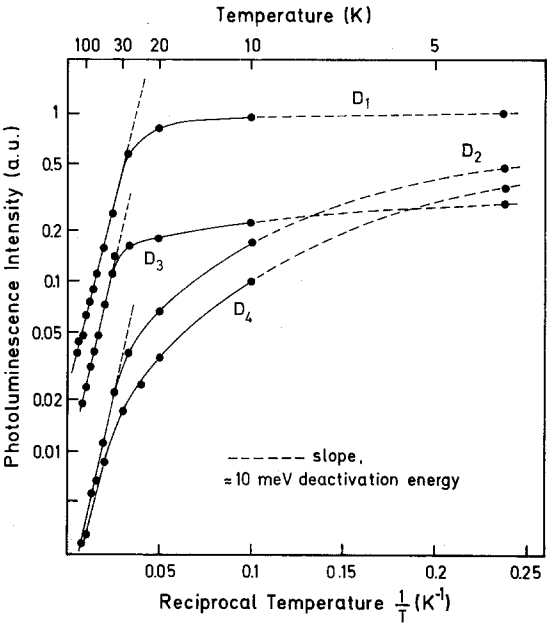

Fig. 10. Temperature dependence of the D1–D4 lines

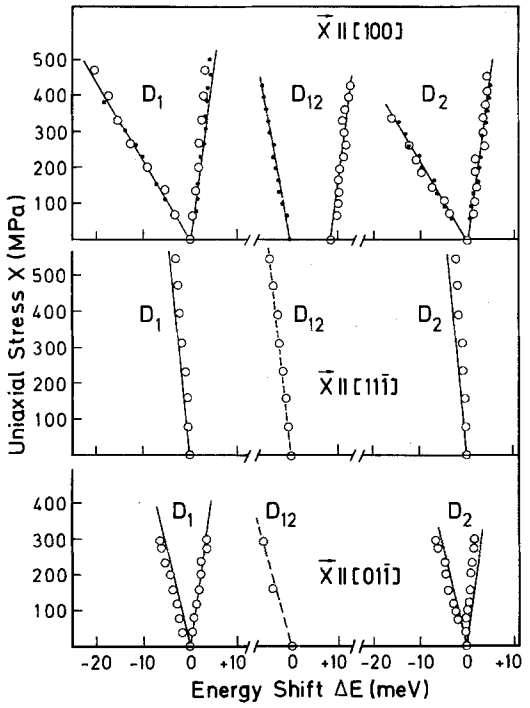

Fig. 11. Stress response of D1, D2, and D12 lines. Open circles and points are experimental as obtained in independent measurements. Solid lines for D1 and D2 are theoretical fits for a tetragonal defect with piezo-optical constants $A_1 = -45.94$ meV/GPa and $A_2 = 11.25$ meV/GPa. Solid and dashed lines for D12 and for the extra line ($\mathbf{X} \parallel [100]$) possibly associated with D12 are optical guides only

they came to the same final expression (1) as we use. Our view of an electron-hole pair simultaneously trapped at a defect where it recombines is formally somewhat different from that of Suezawa et al.; in particular, the localization energy of the loosely bound particle is a result of the interaction with the "nude" defect and the primary, deeply bound carrier.

5. Uniaxial Stress Measurements

The effects of elastic uniaxial stress up to 500 MPa have been studied for the lines D1/D2 and D3/D4 and for the relatively sharp line D6. The line D5 was also measured but is too broad for an unambiguous observation of splitting and shifting effects. The stress was applied along ⟨100⟩, ⟨111⟩, and ⟨110⟩ crystal axes.

Figure 11 summarizes the results for the D1/D2 lines and the D12 line. The experiments were performed on samples exhibiting essentially only one component of D1 and D2 without external stress; i.e. D1 and D2 were not split as, e.g., in Fig. 2. Our results are at variance with the stress response reported by Drozdov et al. [2] who observed merely a shift of the lines but no splitting. They are in agreement with the spectra selectively plotted for several stress values by Suezawa et al. [6, 8]; these authors, however, seem not to have performed a systematic stress study in combination with a quantitative analysis.

For all stress directions, the shift or the splitting of the D1 line is practically identical with that of the D2 line. For $\mathbf{X} \parallel [100]$ and $[01\bar{1}]$ either line is split into two components which do not thermalize but are in a constant intensity ratio. This suggests that the splitting is not due to the lifting of an electronic degeneracy but stems from orientational degeneracy effects of centers of noncubic symmetry. It is important to note that we have recorded identical splittings for stress along $[11\bar{1}]$ (Fig. 11) and $[1\bar{1}1]$, and for stress along $[01\bar{1}]$ (Fig. 11) and [011]. Therefore, the specific stress direction among a given class of directions (considering also directions which are not at all equivalent with respect to the dislocations, as [011] and $[01\bar{1}]$) seems to be irrelevant indicating that the centers are randomly oriented in the crystals. Taking a random orientation for granted we can apply the pertinent linear stress theory on non-cubic centers in cubic crystals as worked out, e.g., by Stoneham [32], Hughes and Runciman [33], and Kaplyanskii [34]. For randomly oriented centers we would observe the full number of stress-induced components for each specific stress direction of a class; it is easily seen that the number of components 2, 1, 2 for stress along ⟨100⟩, ⟨111⟩, ⟨110⟩, respectively, is only consistent with an orientational degeneracy of the centers in tetragonal symmetry. A quantitative analysis is in excellent agreement with this symmetry classification.

Based on Kaplyanskii's work [34] we find that the energy shifts and splittings, the relative intensities and the polarizations of the components are those of a σ-oscillator (i.e. an $A_2 \leftrightarrow B_1$ transition) at a tetragonal center with the piezo-spectroscopic tensor elements $A_1 = -45.94$ meV/GPa and $A_2 = 11.25$ meV/GPa (the A_i refer to differences of corresponding tensor elements of the excited and the ground state). Theoretical stress dependences using these values are plotted in Fig. 11 and are in good agreement with the experimental displacements. Figure 12 depicts, as an example, the spectrum for $X = 406$ MPa along [100] with the observed polarizations indicated. For the A_1 (low energy) component, a σ-oscillator in tetragonal symmetry has relative intensities $I_{\parallel} : I_{\perp}$ of 0:1 for light polarized parallel ($I_{\parallel}$) or perpendicular ($I_{\perp}$) to the stress direction, i.e., this component is purely perpendicular polarized. For the A_2 (high energy) component, the corresponding ratio is 2:1, i.e., this component is parallel *and* perpendicular polarized with a weak preference for parallel polarization. These data are consistent with the experimentally observed polariz-

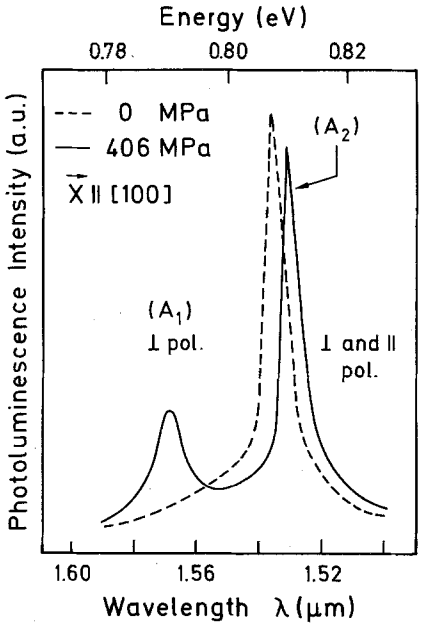

Fig. 12. D1 spectrum at two stress values, $\mathbf{X} \| [100]$, with polarizations indicated. The low-energy component (A_1) is shifted from the zero-stress position by A_1X, the high-energy component (A_2) is shifted by A_2X

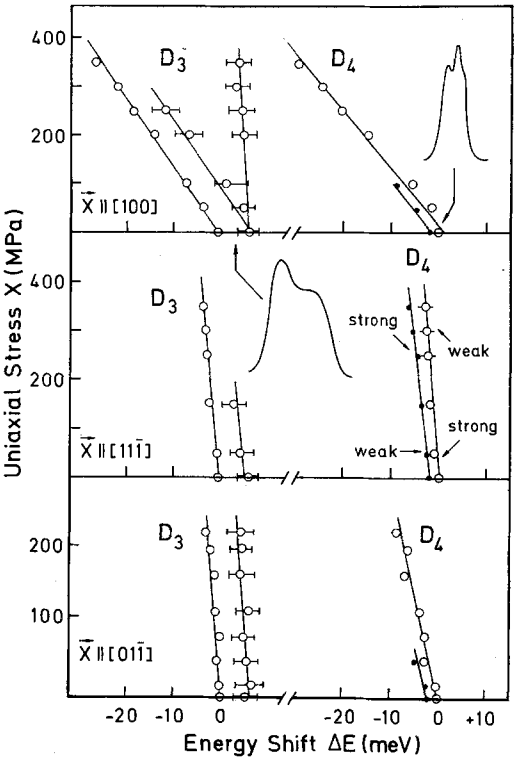

Fig. 13. Dependence of the lines D3 and D4 on stress with the zero-stress finestructure indicated. Solid lines are optical guides

ations together with the total intensity ratio of A_1/A_2 which is theoretically 1:3 and experimentally close to this value (Fig. 12). For stress along [110] and detection of light along [1$\bar{1}$0], the corresponding theoretical ratios are $I_{\|}:I_{\perp}=1:1$ for both components, and experimentally, we observe no polarization, and the intensity ratio of the high-energy to the low-energy component is approximately 1. Therefore, our final conclusion is that we are concerned with transitions at tetragonal defects; the states involved show no electronic stress splitting and correspond to one-dimensional representations. As the splittings for D1 and D2 are practically quantitatively equal these lines may be attributed to transitions at the same defect, and from the stress measurements alone, could involve one common level. We note that the D1/D2 spectra shown by Suezawa et al. [6, 8] for stress along [001] exhibit doublet splittings for each line with equal splitting rates to our measurements. This comparison may corroborate our basic presumption of randomly oriented centers. Actually, the statement of equal population of all equivalent orientations of the tetragonal axis of the defect indicates that the recombination centers are probably not located in the core of a dislocation. Instead, considering also their high symmetry they could rather be deformation produced point defects or other defects in the strain field of the dislocation. In any case, our conclusion is different from that reached by Suezawa et al. who consider the dislocations themselves as the optically active centers.

Next we discuss the dependence of the D3/D4 lines on stress (Fig. 13). This is much more difficult to evaluate than in the former case as the lines are broader and possess an unresolved finestructure. We do not observe any splitting of the lines for the specific stress orientation indicated in Fig. 13. The two unresolved components of the fine-structure shift parallel within experimental error, and for D4 and stress along [111] exchange their relative intensities. For $\mathbf{X} \| [100]$, a high-energy component possibly splits from the two (low-energy) branches of D3 but there is considerable doubt whether this line which is weakly observed at higher stress really develops from D3. We shall assume here that it does not, and may then state that D3 and D4 shift in a similar way with almost identical rates. This supports the close relationship between the associated centers as was previously concluded from other luminescence features.

It is impossible to ascribe such stress response to non-cubic centers which populate at equal probabilities equivalent orientations in the lattice. On the other hand (referring simply to states and not to transitions), A symmetric states of cubic centers would, in fact, not split under uniaxial stress; however, they would shift at *equal* rates [35], also in disagreement with our observa-

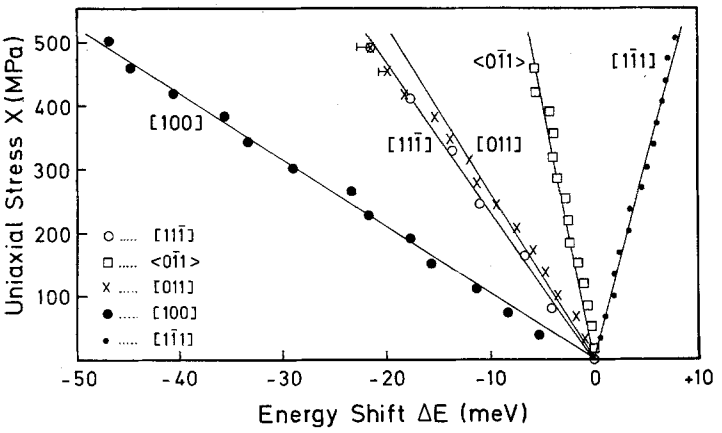

Fig. 14. Stress dependence of the D6 line for five stress directions as indicated

tions. Therefore, it is compulsory to associate D3/D4 with defects which possess certain preferential orientations in the lattice.

This conclusion is compatible with the splitting of the lines under the specific [1$\bar{1}$1] stress (the normal direction of the primary slip plane) as reported by Suezawa and Sumimo [8]. As we have not performed measurements for stress directions other than specified in Fig. 13 we cannot unambiguously deduce the true symmetry of the defects and their preferential alignment.

A similar situation of preferential alignment is encountered for the D6 line (Fig. 14) where we studied the [100]- and two ⟨111⟩- and two ⟨110⟩-directions as indicated in Fig. 14. Important is the observation that each particular stress direction produces no splitting and that the shifts are not the same for [11$\bar{1}$] and [1$\bar{1}$1] or for [011] and ⟨0$\bar{1}$1⟩. The last notation in angular brackets presents an uncertainty, as we do not know the specific direction of the long sample axis in this case except that it is of ⟨110⟩-type and is not [011]. This uncertainly, however, is no problem with respect to the symmetry classification as is discussed below. The different shift rates for stress along specific directions from the same "equivalence"-class make sure that the defect is not randomly oriented. Having more information on hand that for the D3/D4 lines we evaluate the symmetry by assuming the lowest possible symmetry, triclinic, and inspect the piezo-optic tensor for compatibility with higher symmetry groups. In the linear stress response, the energy shifts due to stress are given by the dyadic product of the piezo-optic tensor $\overleftrightarrow{A}$ and the strain tensor $\boldsymbol{\sigma}$. Following the notation of Kaplyanskii [34] we have for the stress induced energy shifts

$$\Delta E = A_1\sigma_{xx} + A_2\sigma_{yy} + A_3\sigma_{zz} + 2A_4\sigma_{xy} + 2A_5\sigma_{yz} + 2A_6\sigma_{xz}$$

and can project out the shifts for the particular experimental stress directions. The results are already contained in [Ref. 34, Table 3] and lead to five linear equations for the A_i. Considering the possible choices for the "uncertain" ⟨110⟩ direction, i.e. the cases [110], [101], [1$\bar{1}$0], [10$\bar{1}$], and [01$\bar{1}$], it is easy to see that severe quantitative contradictions arise in the five equations for each symmetry group higher than triclinic; this is due to the strong restrictions and correlations imposed on the A_i for higher symmetries which cannot be satisfied by the present equations. Therefore, we can unambiguously deduce that the symmetry of the D6 line defect must be triclinic.

Finally, we have also measured the stress response of the D5/D5′ lines. Good measurements are only possible in those cases where D5 appeared as a multiplet of resolved components (Fig. 8) and not as a broad band. Observed are only slight shifts of the multiplet structure with no variations of the spacings between the components but with stress induced changes of the relative intensities. A decision as to the symmetry of the luminescent defect cannot be made.

Our triclinic symmetry classification of the D6 line center is in striking contrast to the tetragonal classification of the D1/D2 line defects. The latter were tentatively associated with deformation produced point defects in the strain field of curved dislocations. The D6 line, on the other hand, appears in crystals of high stacking fault densities. If the line were due to the recombination of electrons and holes simply localized at stacking fault atoms one would rather expect to observe higher symmetric luminescence features. The nearest neighbors of an atom in the stacking fault form a tetrahedron, the next-nearest shell of neighbors is hexagonal and there is at least the preferential c-axis parallel to ⟨111⟩. The triclinic symmetry of the D6 line center suggests a more complex optically active defect. The simultaneous appearance of this low symmetry defect with high stacking fault densities remains not understood and needs further experimental work.

The D3 and D4 defects seem to be much closer related to the D5 and D6 centers than D1 and D2 as they preferentially form on annealing the straight dislocations and stacking faults and are also energetically very close to the D5/D6 lines. Moreover, they are either preferentially oriented or have triclinic symmetry like the D6 defect. One may also recall that the D3/D4, D5, and D6 lines, although possessing largely differing halfwidths, are all much broader than the D1/D2 lines. All these features conspire to suggest a close relation among the higher-energy luminescence lines D3, D4, D5, and D6 set off against the contrasting features of the low-energy luminescence lines D1 and D2.

6. Summary

The paper presents a study of photoluminescence lines which emerge in plastically deformed silicon crystals. We show that the lines D1/D2 and D3/D4 are related to the presence of "relaxed" dislocations which have been frozen in under low-shear stress. These lines appear as pairs in many respects. Most striking is their identical stress response. However, D1/D2 are emitted by tetragonal centers which are randomly distributed over all equivalent orientations and are, therefore, not regarded as the most characteristic optical testimonies of the dislocations. They might originate in deformation-induced point defects located in the strain region of curved dislocation. D3/D4 have either triclinic symmetry or, if the symmetry is higher, are preferentially aligned in the lattice. New lines D5 and D6 are produced when the standard high-temperature, low-stress deformation is followed by low-temperature, high-stress deformation. Combining the results of transmission electron microscopy and of our photoluminescence measurements, we propose that line D5 is due to straight dislocations and D6 is due to stacking faults. The D6 optical center has triclinic symmetry. Both new lines disappear on annealing the samples generating then preferentially the D3/D4 lines. The relaxation occurs close to 300 °C. These features lead us to suggest that the D3/D4 photoluminescence is much more characteristic of the dislocations themselves than the D1/D2 emission lines.

Acknowledgements. We are grateful to D. Bäuerle (Universität Linz, Austria), L.C. Kimerling (AT&T Bell Laboratories, USA), E. Bauser and coworkers (Max-Planck-Institut für Festkörperforschung, Stuttgart), and H. Conzelmann (Physikalisches Institut, Teil 4, Universität Stuttgart) for the gift of samples or for placing particular PL spectra at our disposal. H. Gottschalk (II. Physikalisches Institut, Universität Köln) contributed TEM results on dislocation morphology and annealing of deformed crystals and M. Kolbe, II. Physikalisches Institut, Universität Köln, deformed a number of crystals. We are also grateful to D. Gwinner, Technische Universität Clausthal, now with Degussa AG, Hanau, for the hydrogenation of two of our samples. One of the authors (R.S.) is largely indebted to K. Thonke, Physikalisches Institut, Teil 4, Universität Stuttgart, for discussions on part of the stress measurements.

References

1. N.A. Drozdov, A.A. Patrin, V.D. Tkachev: Pis'ma Zh. Eksp. Teor. Fiz. **23**, 651 (1976); Sov. Phys. JETP Lett. **23**, 597 (1976)
2. N.A. Drozdov, A.A. Patrin, V.D. Tkachev: Phys. stat. sol. (b) **83**, K137 (1977)
3. R.H. Uebbing, P. Wagner, H. Baumgart, H.J. Queisser: Appl. Phys. Lett. **37**, 1078 (1980)
4. D. Gwinner, R. Labusch: Phys. stat. sol. (a) **65**, K99 (1981)
5. M. Suezawa, Y. Sasaki, Y. Nishina, K. Sumino: Jpn. J. Appl. Phys. **20**, L537 (1981)
6. M. Suezawa, K. Sumino, Y. Nishina: Jpn. J. Appl. Phys. **21**, L518 (1982)
7. M. Suezawa, K. Sumino: Phys. stat. sol. (a) **78**, 639 (1983)
8. M. Suezawa, K. Sumino: J. Phys. (Paris) **44**, C4–133 (1983) (Proc. Intern. Symp. Structure and Properties of Dislocations in Semiconductors, Aussois, France 1983)
   M. Suezawa, Y. Sasaki, K. Sumino: Phys. stat. sol. (a) **79**, 173 (1983)
9. N.A. Drozdov, A.A. Patrin, V.D. Tkachev: Phys. stat. sol. (a) **64**, K63 (1981)
10. Y.A. Osip'yan, A.M. Rtishchev, E.A. Shteinman, E.B. Yakimov, N.A. Yarykin: Zh. Eksp. Teor. Fiz. **82**, 509 (1982); Sov. Phys. JETP **55**, 294 (1982)
11. D. Gwinner, V.V. Kveder: Private communication
12. D. Gwinner: J. Phys. (Paris) **44**, C4–141 (1983)
13. H. Alexander, C. Kisielowski-Kemmerich, E.R. Weber: Physica **116**B, 583 (1983) (Proc. 12th Intern. Conf. Defects in Semiconductors, Amsterdam, The Netherlands, 1982)
14. R. Sauer, J. Weber: *Lecture Notes in Physics* **175**, 120 (Springer, Berlin, Heidelberg, New York 1983) (Proc. Intern. School Defect Complexes in Semiconductor Structures, Matrafüred, Hungary 1982)
15. E.R. Weber, H. Alexander: J. Phys. (Paris) **44**, C4–319 (1983)
16. K. Wessel, H. Alexander: Philos. Mag. **35**, 1523 (1977)
17. See, for literature, J.C. Hensel, T.G. Phillips, G.A. Thomas: *Solid State Physics* **32**, 87 (Academic Press, New York 1977) T.M. Rice: *Solid State Physics* **32**, 1 (Academic Press, New York 1977)
18. E. Weber, H. Alexander: Inst. Phys. Conf. Ser. **31**, 266 (1977)
19. Spectrum and sample history by courtesy of H. Conzelmann (private communication)
20. Sample and sample data from L.C. Kimerling (AT&T Bell Laboratories, USA)
21. Samples from D. Bäuerle (University of Linz, Austria); description of crystal growth in D. Bäuerle, P. Irsigler, G. Leyendecker, H. Noll, D. Wagner: Appl. Phys. Lett. **40**, 819 (1982)
22. K. Köhler, W. Appel, E. Bauser (Max-Planck-Institut für Festkörperforschung, Stuttgart) (private communication)
23. Same treatment as in [11 and 12]
24. Same treatment as in [25]
25. B. Pohoryles: Phys. stat. sol. (a) **67**, K75 (1981)
26. H. Alexander: In *Dislocations: Structure de coeur et propriétés physiques*, ed. by P. Veyssière, L. Kubin, and J. Castaing, Editions de CNRS (1984) (in press)
27. H. Alexander, K. Wessel: J. Phys. (Paris) **39**, C2–114 (1978)
28. K.-H. Küsters: Unpublished work
    H. Gottschalk, 10th Intern. Congress Electr. Microsc. (Hamburg, 1982) p. 527
29. H. Teichler: J. Phys. (Paris) **40**, C6–43 (1979)
30. R. Sauer, J. Weber: Physica **116**B, 195 (1983)
31. See, for details, the discussion in K. Thonke, J. Weber, J. Wagner, R. Sauer: Physica **116**B, 252 (1983)
32. A.M. Stoneham: *Theory of Defects in Solids* (Clarendon Press, Oxford 1975)
33. A.E. Hughes, W.A. Runciman: Proc. Phys. Soc. **90**, 827 (1967)
34. A.A. Kaplyanskii: Opt. Spectrosc. **16**, 329 (1964)
35. A.A. Kaplyanskii: Opt. Spectrosc. **16**, 557 (1964)